Progress In Electromagnetics Research Letters, Vol. 79, 25–31, 2018

Modified CMRC LPF Using Novel Fractal Patches

Mohammed E. Yassin[1, 2, *], Hesham A. Mohamed[3], Esmat A. F. Abdallah[3], and Hadia S. El-Hennawy[2]

Abstract—A modified compact microstrip resonance cell (CMRC) low pass filter (LPF) with ultrawide and deep stopband using novel fractal patches is presented. The proposed filter has a low insertion loss in the passband, good selectivity, ultrawide and deep stopband. The experimental results show a 3-dB cutoff frequency of 2.85 GHz and out-of-band rejection up to 67 GHz with 181.5% relative stopband bandwidth Low pass microstrip filters, ultrawide band, compact microstrip resonance cell (CMRC), fractal.

1. INTRODUCTION

Recently, the increasing need for high data rate and compactness in addition to the increasing congestion in the traditional spectrum are pushing the most of modern communication systems to be developed in high SHF, EHF, Ka, Q, U and V bands for many applications such as 5G communication system [1], 28 GHz RFID [2, 3], hyperspectral microwave radiometer [4], synthetic aperture radar [5], inter-satellite communications [6], Wireless Gigabit Alliance(WiGig) [7], W-band imaging radiometer system [8], and the millimeter-wave satellite communications [9–11], radar systems [12, 13]; therefore, low pass filters with an extra ultrawide stopband bandwidth are in demand to prevent inter-modulation with the new systems operating bands.

The compact microstrip resonance cell (CMRC) was proposed for the first time in [14], and it consists of microstrip triangular photonic bandgap (PBG) cells connected by narrow lines as shown in Fig. 1. The transverse and longitudinal narrow strips lead to an increase in the series inductance, while the triangular patches and the microstrip gaps between the triangular patches and the microstrip lines lead to an increase in the shunt capacitance, magnifying slow wave effect whilst keeping the size compact. It suffers from the narrow stop bandwidth and wide transition. A vast amount of research was undertaken in order to overcome these disadvantages. Reference [15] presents a filter of two cascaded improved double folded spiral compact microstrip resonant cells (DSCMRC) with two parallel open-ended stubs. It consists of four folded lines instead of four triangular patches in [14], which increases the series inductance and shunt capacitance. Furthermore, two parallel open-ended 60-degree sector stubs are used to further extend the out of band rejectionby adding extra transmission zeros in the stopband, which achieves 21 GHz stopband (from 4 GHz to 25 GHz).

In [16], a funnel patch resonator (FPR) is placed between two triangle patch resonators (TPR) symmetrically about the center of a high impedance line. The combination of the three cascaded resonators achieves 5.92 GHz stopband (from 5.88 GHz to 11.8 GHz), while in [17], three multimode resonators with different sizes are placed in either side of the narrow width microstrip line. Each multimode resonator can introduce its transmission zeroes in the stopband. This achieves 21.17 GHz stopband (from 2.83 GHz to 24 GHz). Two cascaded novel cells in [18] are used, and each consists of

Received 16 July 2018, Accepted 7 September 2018, Scheduled 30 September 2018

* Corresponding author: Mohammed Ezzat Yassin (el_be7ery@yahoo.com).

[1] Akhbar Elyom Academy, 6th of October City, Egypt. [2] Faculty of Engineering, Ain Shams University, Cairo, Egypt. [3] Electronics Research Institute, Giza, Egypt.

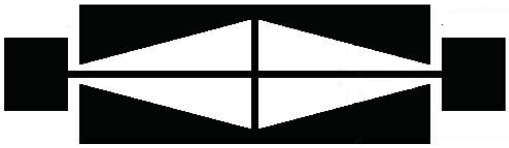

Figure 1. Original CMRC structure [14].

CMRC resonators with four open microstrip stub lines, which are embedded in the microstrip line to achieve a wider stopband. The filter achieves 34.9 GHz stopband (from 5.1 GHz to 40.0 GHz). In [19], a low pass filter consisting of two unequally sized pairs of quad-mode resonators is presented, and each resonator consists of a folded half-wavelength resonator and three parallel open stubs. The quad-mode resonators filter achieves 18.3 GHz stopband (from 3.1 GHz to 21.4 GHz). The previously presented papers achieve a wider stopband than the original CMRC filter. However, they have much difficulty to prevent inter-modulation with the new systems with high frequency operating bands.

To solve this problem, the proposed filter consists of half of a traditional compact microstrip resonance cell (CMRC) [14], with four openended stubs and two unequally sized novel fractal patches in the other half to act as dual behavior resonators (DBRs) to combine the slow wave property and compact size of CMRC with the additional transmission zeros of the DBR and bandwidth extension of the stubs to achieve an ultrawide and deep stopband bandwidth [20]. The paper is organized as follows. The design and structure are given in Section 2. Section 3 presents the simulation results, while Section 4 gives the measured results after fabrication. Finally, the conclusions are introduced in Section 5.

2. DESIGN AND STRUCTURE

In order to achieve a low pass filter with a compact size, ultra-wide deep stopband and sharp roll-off, a modified CMRC LPF using novel fractal patches is presented in this paper. The filter was designed on a Rogers 5880 substrate with a relative dielectric constant of 2.2, substrate thickness of 0.508 mm and loss tangent of 0.0009. Fig. 2 shows the proposed filter design, which consists of two traditional triangle taper resonance cells in one side of the transverse connecting narrow width transmission line which has almost the same performance of the complete CMRC structure, while two differently sized circular fractal patches are present on the other half. Each fractal consists of a main circular patch and additional small circular patches at the edges. The two fractals act as a dual behavior resonator to obtain additional transmission zeros in the stopband. Each fractal resonates at a certain frequency in addition to enhancing the low suppression bands of the entire stopband. Also, four open ended stubs are used to extend the stopband by adding new transmission zeros without increasing the circuit size. The main dimensions are given in Table 1, all dimensions in millimeter.

Table 1. Circuit dimensional parameters.

Parameter	C_l	L	W	C_{d1}	C_{d2}	a_{11}	a_{12}	a_{13}	a_{21}
Value (mm)	17.6	2.4	0.15	7.6	2.1	1.35	0.2	0.05	2.9
Parameter	a_{22}	a_{23}	X_1	X_2	Y_1	Y_2	T_1	T_2	W_{50}
Value (mm)	0.15	0.05	2.4	1.8	0.8	0.8	3.2	3.8	1.6

Figure 3 shows that the distributive equivalent circuit of the filter which is built up and simulated by using Advanced Design System (ADS) software. The triangle patches are represented as microstrip tapers and the fractal circles as radial stub with the same area, while resistors are added to represent the losses.

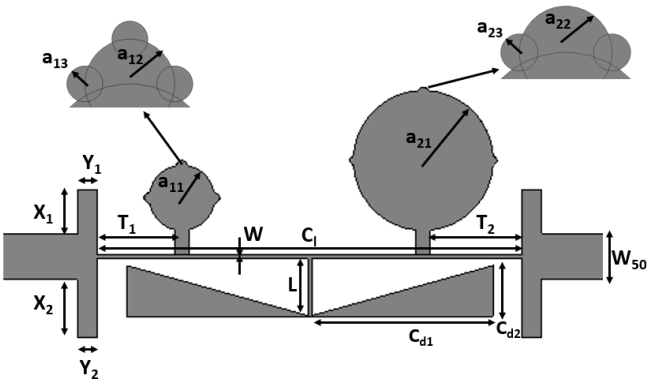

Figure 2. The design of proposed lowpass filter.

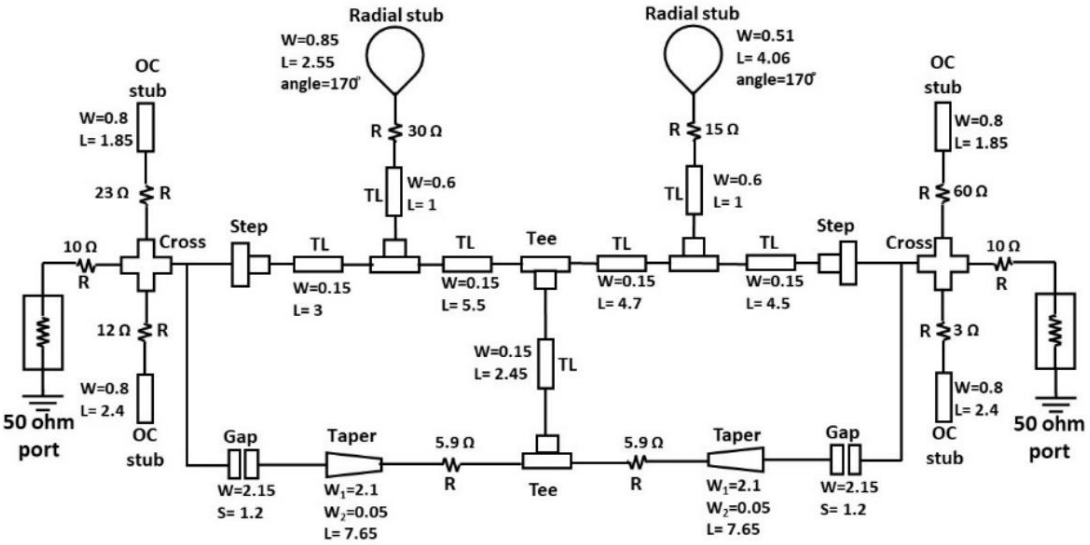

Figure 3. The distributive equivalent circuit (all dimensions in mm).

3. SIMULATION RESULTS

Figure 4 shows the results of the proposed filter simulated using Computer Simulation Technology (CST) and the distributive equivalent circuit simulated by using Advanced Design System (ADS) circuit and momentum simulations. A good agreement is between the simulation results by the two software packages.

Figure 5(a) illustrates the response of the filter simulated by Computer Simulation Technology (CST) with only half of the CMRC, which shows a single transmission zero in the stopband at 3.1 GHz, with a wide transition. Fig. 5(b) exhibits filter characteristics with the two differently sized fractal patches which improves the stopband performance by adding a transmission zero at 5.8 GHz. The four open-ended stubs cause the stopband bandwidth to be extended beyond 16 GHz, Fig. 5(c).

The length of the transverse narrow connecting line (C_l), the gap width and the triangle taper size determine the resonance frequency of the CMRC, while decreasing the transverse narrow connecting line (w) enhances the return loss especially in the frequency range of 5 GHz to 10 GHz. The main circles' sizes of the fractal patches determine the location of its transmission zeros while smaller circles are added to the main fractal circles to enhance the return loss in the stopband. The lengths of the four open circuit stubs are adjusted to enhance the return loss in the range from 16 GHz to 43 GHz of the stopband.

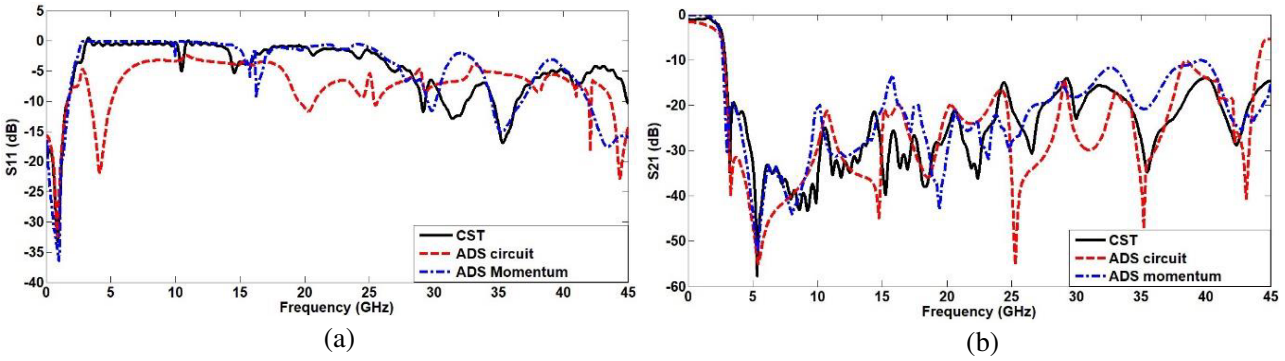

Figure 4. The simulation results using CST and ADS (a) $|S_{11}|$, and (b) $|S_{21}|$.

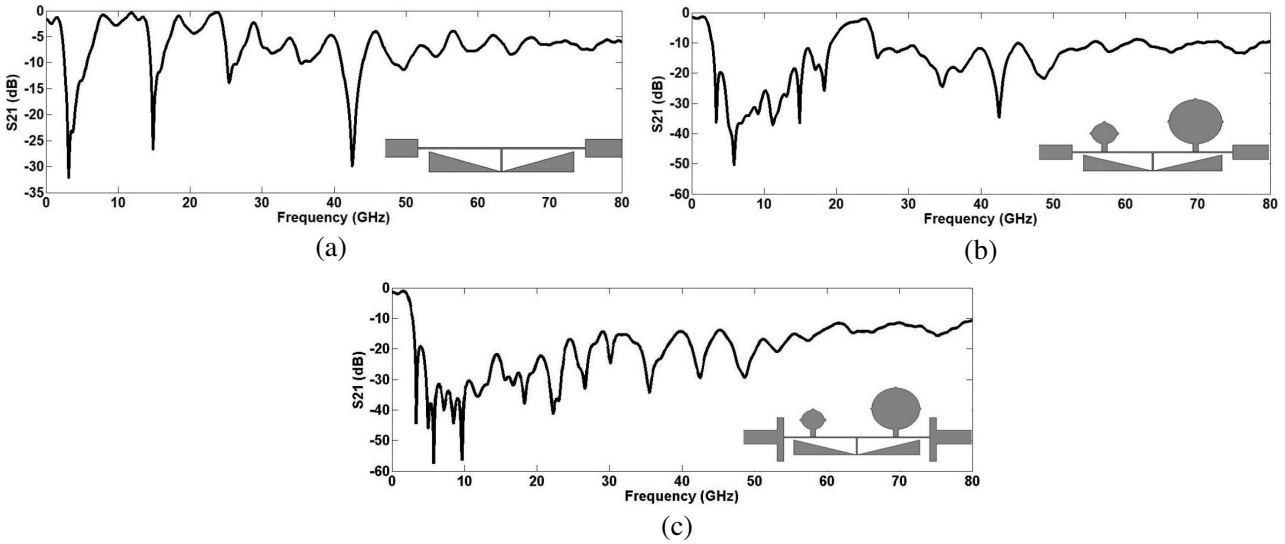

Figure 5. The simulated $|S_{21}|$ parameter using CST of: (a) half CMRC, (b) half CMRC with the two fractals, and (c) half CMRC with the two fractals and four open stubs.

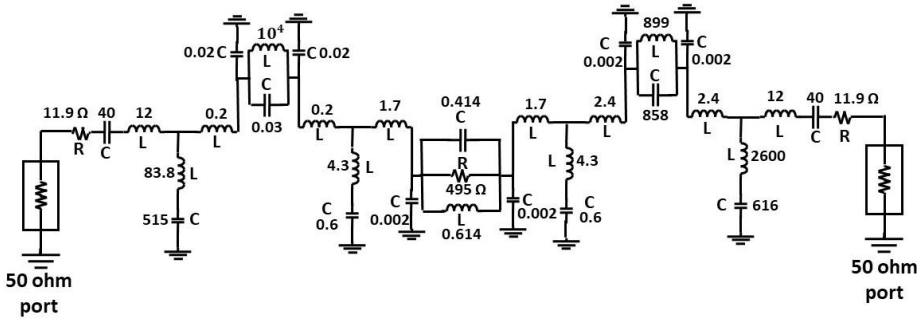

Figure 6. The lumped elements equivalent circuit (the capacitors in pF and inductors in nH).

Figure 6 shows the lumped element equivalent circuit of the final filter design, while Fig. 7 shows the comparison between the simulation results of the filter design and equivalent circuit. The simulated results show that the insertion loss is less than 1 dB in the passband from DC to 2.6 GHz with 3 dB cutoff frequency at 2.8 GHz and from -3 dB to -20 dB transition of 0.6 GHz. The proposed filter achieves -10 dB bandwidth from 3.2 GHz to 80 GHz with -20 dB suppression from 5.7 GHz to 30.5 GHz with relative stopband bandwidth (RSB) of 185%.

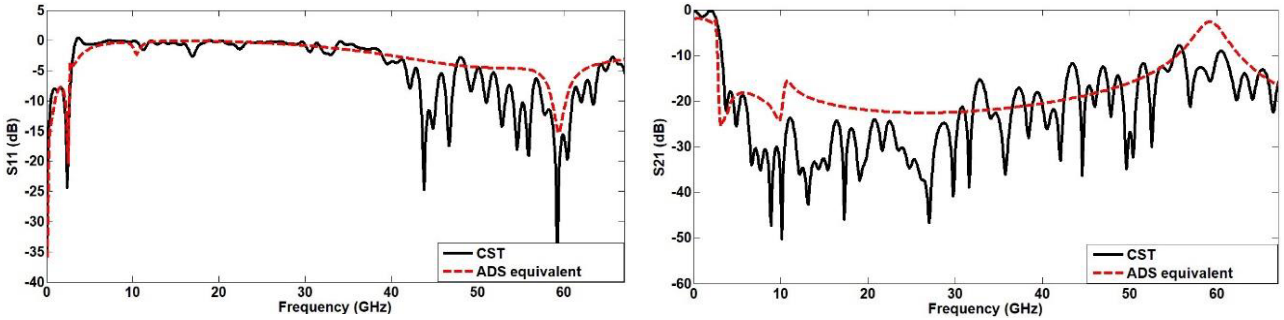

Figure 7. The simulation results of the filter using CST and the equivalent circuit using ADS (a) $|S_{11}|$, and (b) $|S_{21}|$.

4. MEASUREMENT RESULTS

On the basis of the analysis above, the filter has been fabricated using the photolithographic technique. Fig. 8 shows a photograph of the fabricated LPF. The total filter size is $22.2 * 10.5\,\text{mm}^2$, which equals $0.3\lambda g \times 0.14\lambda g$, where λg is the guided wavelength of microstrip line at the 3-dB cutoff frequency.

The reflection coefficients were measured using a ROHDE&SCHWARZ ZVA 67 vector network analyzer which limits the measurements to 67 GHz through 1.85 mm end-launch mm-wave connectors. The simulated and measured results are shown in Fig. 9. The differences between the simulation and measurement results are probably due to the fabrication tolerance and mm-wave connector effect. The measurements show that the insertion loss is less than 1.5 dB in the passband from DC to 2.7 GHz with 3 dB cutoff frequency at 2.85 GHz and 0.55 GHz transition from -3 dB to -20 dB. The proposed filter achieves -10 dB bandwidth from 3.3 GHz to 67 GHz with -20 dB suppression from 3.5 GHz to 67 GHz. Table 2 shows the comparison between the proposed filter and other literature filters.

Table 2. Performance comparison with other CMRCs.

Ref	ε_r	3-dB cutoff frequency (GHz)	Stopband (-10 dB) (GHz)	RSB (%)	Size (mm)	Size ($\lambda g \times \lambda g$)
[16]	3.5	3.5	4–25	145	$20 * 14.4$	$0.43 * 0.31$
[17]	4.4	5.55	5.88–11.8	67	$9.4 * 8$	$0.36 * 0.31$
[18]	3.5	1.8	2.6–24	158	$9 * 11.7$	$0.09 * 0.11$
[19]	3.5	4.8	5.1–40	155	$7.3 * 3.7$	$0.2 * 0.1$
[20]	3.5	2.2	3.1–24.4	133	$13.2 * 14.2$	$0.16 * 0.17$
This work	2.2	2.85	3.3–67	181.5	$22.2 * 10.5$	$0.31 * 0.15$

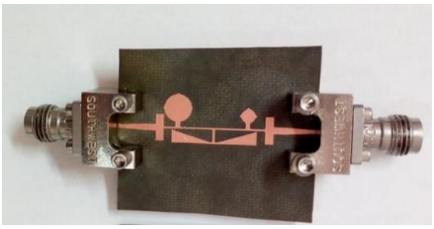

Figure 8. Photograph of fabricated LPF.

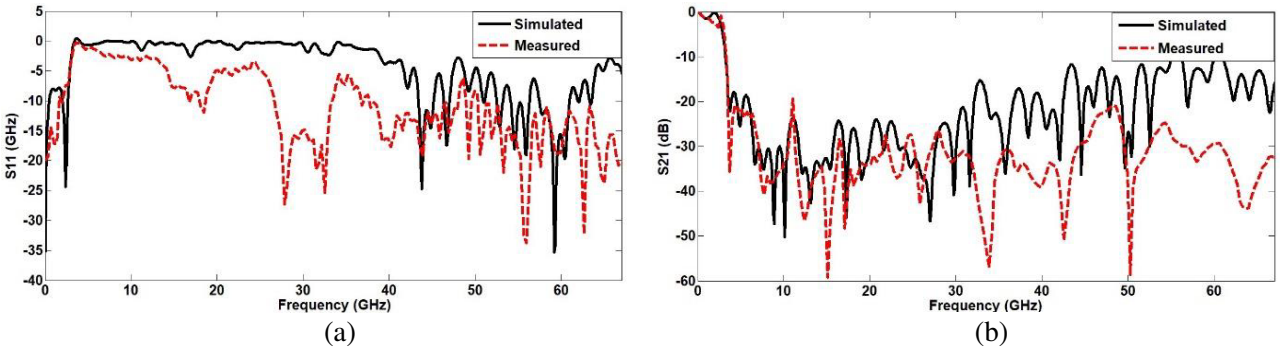

Figure 9. The measured and simulated results (a) $|S_{11}|$, and (b) $|S_{21}|$.

5. CONCLUSION

A modified compact microstrip resonance cell (CMRC) low pass filter (LPF) using novel fractal patches is proposed. The fractal patches produce additional transmission zeros to the stop-band while the open-ended stubs cause an extension in the stopband achieving a compact ultrawide and deep stopband filter with good selectivity and low insertion loss in the passband. The results show −10 dB bandwidth from 3.3 GHz to 67 GHz with 181.5% relative stopband bandwidth. The 3-dB cutoff frequency is 2.85 GHz, less than 1.5 dB insertion loss in the passband, 0.55 GHz transition from −3 dB to 20 dB, and −20 dB suppression from 3.5 GHz to 67 GHz, so that the filter can be expected to suppress unwanted harmonics and prevent inter-modulation with the new systems with high frequency operating bands.

REFERENCES

1. Khan, R., A. Abdullah Al-Hadi, and P. J. Soh, "Efficiency of millimeter wave mobile terminal antennas with the influence of users," *Progress In Electromagnetics Research*, Vol. 161, 113–123, 2018.
2. Lischer, S., M. Heiss, M. Landwehr, and W.-Joachim Fischer, "A 24 GHz RFID system-on-a-chip with on-chip antenna, compatible to ISO 18000-6C/EPC CIG2," *IEEE International Conference on Microwaves, Communications, Antennas and Electronic Systems (COMCAS)*, 1–4 Tel Aviv, Israel, Nov. 2–4, 2015.
3. Attaran, A., R. Rashidzadeh, R. Muscedere, "Rotman lens combined with wide bandwidth antenna array for 60 GHz RFID applications," *International Journal of Microwave and Wireless Technologies*, 1–7, Jul. 2015.
4. Xie, Y., J. Chen, D. Liu, C. Lv, K. Liu, and J. Miao, "Development and calibration of a K-band ground-based hyperspectral microwave radiometer for water vapor measurements," *Progress In Electromagnetics Research*, Vol. 140, 415–438, 2013.
5. Kurniawan, F., J. T. Sri Sumantyo, K. Ito, H. Kuze, and S. Gao, "Patch antenna using rectangular centre slot and circular ground slot for circularly polarized synthetic aperture radar (CP-SAR) application," *Progress In Electromagnetics Research*, Vol. 160, 51–61, 2017.
6. Liu, Y., J. Xu, Y.-Y. Wei, X. Xu, F. Shen, M. Huang, T. Tang, W.-X. Wang, Y.-B. Gong, and J. Feng, "Design of a V-band high-power sheet-beam coupled-cavity traveling-wave tube," *Progress In Electromagnetics Research*, Vol. 123, 31–45, 2012.
7. Wang, D. and C. Hou Chan, "Multiband antenna for WiFi and WiGig communications," *IEEE Antennas and Wireless Propagation Letters*, Vol. 15, 309–312, 2015.
8. Kim, W.-G., N.-W. Moon, J. Kang, and Y.-H. Kim, "Loss measuring of large aperture quasi-optics for W-band imaging radiometer system," *Progress In Electromagnetics Research*, Vol. 125, 295–309, 2012.

9. Mener, S., R. Gillard, and L. Roy, "A dual-band dual-circular-polarization antenna for Ka-band satellite communications," *IEEE Antennas and Wireless Propagation Letters*, Vol. 16, 274–277, 2016.
10. Trinh-Van, S., H. B. Kim, G. Kwon, and K. C. Hwang, "Circularly polarized spidron fractal slot antenna arrays for broadband satellite communications in Ku-band," *Progress In Electromagnetics Research*, Vol. 137, 203–218, 2013.
11. De Sanctis, M., E. Cianca, T. Rossi, et al., "Waveform design solutions for EHF broadband satellite communications," *IEEE Communications Magazine*, Vol. 53, No. 3, 18–23, 2015.
12. Attaran, A., R. Rashidzadeh, and A. Kouki, "60 GHz low phase error Rotman lens combined with wideband microstrip antenna array using LTCC technology," *IEEE Transactions on Antennas and Propagation*, Vol. 64, No. 12, 5172–5180, Dec. 2016.
13. Attaran, A. and S. Chowdhury, "Fabrication of a 77 GHz Rotman lens on a high resistivity silicon wafer using lift-off process," *International Journal of Antennas and Propagation*, 1–9, article ID: 471935, 2014.
14. Xue, Q., K. M. Shum, and C. H. Chan, "Novel 1-D microstrip PBG Cells," *IEEE Microwave and Guided Wave Letters*, Vol. 10, 403–405, 2000.
15. Li, K., M. Zhao, Y. Fan, Z. B. Zhu, and W.-Z. Cui, "Compact lowpass filter with wide stopband using novel double-folded SCMRC structure with parallel open-ended stub," *Progress In Electromagnetics Research*, Vol. 36, 77–86, 2013.
16. Raphika, P. M., P. Abdulla, and P. M. Jasmine, "Compact lowpass filter with a sharp roll-off using patch resonators," *Microwave and Optical Technology Letters*, Vol. 56, 2534–2536, 2014.
17. Li, Q., Y. Zhang, and Y. Fan, "Compact ultra-wide stopband low pass filter using multimode resonators," *Electronics Letters*, Vol. 51, 1084–1085, 2015.
18. Tang, W., X. B. Yang, and L. H. Zuo, "A compact lowpass filter with ultra-wide stopband using novel resonance cell," *Microwave and Millimeter Wave Circuits and System Technology (MMWCST)*, 1–3, Chengdu, China, Apr. 19–20, 2012.
19. Li, Q., Y. Zhang, D. Li, and K. Xu, "Compact low-pass filters with deep and ultra-wide stopband using tri- and quad-mode resonators," *IET Microwaves, Antennas & Propagation*, Vol. 11, 743–748, 2017.
20. Chang, Y., W. Feng, and W. Che, "Dual-band bandpass filters with high isolation using coupled lines," *International Journal of Electronics*, Vol. 103, 372–383, 2015.